J Mater Sci: Mater Electron (2021) 32:28223–28233

$LiNbO_3$-coated $Li_{1.2}Mn_{0.54}Ni_{0.13}Co_{0.13}O_2$ as a cathode material with enhanced electrochemical performances for lithium-ion batteries

Jie Wang[1], Kewei Wu[1], Changsheng Xu[1], Xuebu Hu[1,*], and Lei Qiu[1]

[1] *College of Chemistry and Chemical Engineering, Chongqing University of Technology, Chongqing 400054, China*

Received: 20 August 2021
Accepted: 7 October 2021
Published online: 15 October 2021

ABSTRACT

Lithium-rich manganese-based cathode materials have become one of the most concerned cathode materials for high-energy lithium-ion batteries. In order to improve its electrochemical performance, $Li_{1.2}Mn_{0.54}Ni_{0.13}Co_{0.13}O_2$ with different content $LiNbO_3$ coatings was synthesized by mechanical ball milling. The morphology, microstructure, and electrochemical properties of the samples were investigated by X-ray diffraction, scanning electron microscope, transmission electron microscope, galvanostatic charge/discharge, electrochemical impedance spectroscopy, and cyclic voltammetry. The results show that $LiNbO_3$ coating not only protects the cathode material from the corrosion of electrolyte and HF but also improves the migration rate of Li^+ in the interface region. Notably, the 5 wt% $LiNbO_3$-coated $Li_{1.2}Mn_{0.54}Ni_{0.13}Co_{0.13}O_2$ exhibits capacity retention of 89.9% under 0.1 C after 100 cycles. Besides, it has a higher discharge capacity than $Li_{1.2}Mn_{0.54}Ni_{0.13}Co_{0.13}O_2$ at different rates. $LiNbO_3$ coating is an effective way to improve its cycle stability and rate performance of $Li_{1.2}Mn_{0.54}Ni_{0.13}Co_{0.13}O_2$.

1 Introduction

Lithium-ion batteries have been widely used in portable devices, electric vehicles, and hybrid vehicles owing to high voltage, high capacity, good safety performance, and environmental friendliness [1–3]. The capacity and stability of cathode materials have become important factors limiting the further development of lithium-ion batteries [4, 5]. Lithium-rich manganese-based cathode material has attracted the interest of many researchers because of its high discharge capacity (> 250 mAh g^{-1}), low cost, and environmental friendliness [6]. More important, it combines the stability of $LiCoO_2$, high capacity of $LiNiO_2$, and low cost of $LiMnO_2$ [4, 7] and its good safety performance has attracted the attention of researchers.

However, there are still many problems with lithium-rich manganese-based cathode, such as low initial efficiency, rapid discharge voltage drop during cycling, poor thermal stability, and cycle performance [8]. The foremost reason for these

Address correspondence to E-mail: xuebu@cqut.edu.cn

https://doi.org/10.1007/s10854-021-07199-1

shortcomings are due to its poor stability of layered structure during charge/discharge which changes from layered to spinel phase [9]. In order to solve these issues, the surface modification has been certified to be an availably way to protect the cathode materials surface from electrolyte erosion, which can significantly enhance the structural stability during cycling [10]. Zhou et al. synthesized Li_2SiO_3-coated $Li_{1.2}Mn_{0.54}Ni_{0.13}Co_{0.13}O_2$ which greatly enhanced initial coulombic efficiency, cycle stability, and rate capability [11]. He et al. improved initial coulombic efficiency and cycle stability of $Li_{1.2}Mn_{0.54}Ni_{0.13}Co_{0.13}O_2$ cathodes by $SmPO_4$ as a coating material [12]. As a fast lithium-ion conductor, the conductivity of $LiNbO_3$ is approximately 10^{-6} S cm^{-1}, which can increase the diffusion rate of lithium ions during charge/discharge process. At the same time, $LiNbO_3$ has better thermal and chemical stability.

In this study, $Li_{1.2}Mn_{0.54}Ni_{0.13}Co_{0.13}O_2$ is coated with a layer of $LiNbO_3$ particles. The $LiNbO_3$ layer can serve two functions: (1) preventing the direct contact between $Li_{1.2}Mn_{0.54}Ni_{0.13}Co_{0.13}O_2$ and the electrolyte, thereby reducing the corrosion of the cathode material and (2) reducing lithium-ion transfer barrier at the electrode–electrolyte interface. As a consequence, cycle stability and rate performance of $Li_{1.2}Mn_{0.54}Ni_{0.13}Co_{0.13}O_2$ are obviously improved via $LiNbO_3$ surface modification.

2 Experiment

2.1 Synthesis of $LiNbO_3$

$NbCl_5$ was dissolved in 35% H_2O_2 solution until completely dissolved, $C_2H_3LiO_2{\cdot}2H_2O$ and citric acid were slowly added and violently stirred, and then the solvent completely evaporated at 65 °C. The resulting colloidal substance was dried and ground. Finally, $LiNbO_3$ (LNO) was obtained by calcination at 600 °C.

2.2 Synthesis of $Li_{1.2}Mn_{0.54}Ni_{0.13}Co_{0.13}O_2$ and $LiNbO_3$-coated $Li_{1.2}Mn_{0.54}Ni_{0.13}Co_{0.13}O_2$

Stoichiometric amounts of $MnSO_4{\cdot}H_2O$, $NiSO_4{\cdot}6H_2O$, and $CoSO_4{\cdot}7H_2O$ (the molar ratio was 4:1:1) were dissolved in deionized water to form a mixed solution with a total metal concentration of 2 mol L^{-1}. The mixed solution was added to the reactor through a peristaltic pump in nitrogen as a protective gas. At the same time, Na_2CO_3 solution was added to the reactor as a precipitant, and $NH_3{\cdot}H_2O$ solutions were used to adjust the pH around 7.5. After 12 h, the sediment was filtered, washed with deionized water, and dried. The as-obtained precursor $Mn_{4/6}Ni_{1/6}Co_{1/6}CO_3$ was mixed with Li_2CO_3 (5 mol% excess) and pre-sintered at 500 °C for 5 h and then calcined at 900 °C for 12 h to prepare $Li_{1.2}Mn_{0.54}Ni_{0.13}Co_{0.13}O_2$ (LMNCO) material. The mixtures of $LiNbO_3$ and $Li_{1.2}Mn_{0.54}Ni_{0.13}Co_{0.13}O_2$ were milled via planet type ball mill and then sintered at 500 °C for 5 h. Different weight contents of LNO-coated LMNCO (1 wt% LNO-LMNCO, 3 wt% LNO-LMNCO, and 5 wt% LNO-LMNCO) were obtained.

2.3 Material characterization

X-ray diffraction (XRD, Cu-Ka, λ = 0.154056 nm) was applied to analyze phase composition and lattice structure of all samples at a voltage of 40 kV, a current of 30 mA, and the scanning 2θ range angle from 10° to 80°. Scanning electron microscope (SEM, Quanta FEI) and transmission electron microscope (TEM, FEI TecnaiG2 F20) were used to observe the morphology and microstructure of all samples. The content of dissolved Ni, Co, and Mn in the electrolyte was detected by Inductively coupled plasma mass spectrometry (ICP-MS).

2.4 Electrochemical measurements

The positive electrode material, acetylene black, and polyvinylidene fluoride were mixed in a mass ratio of 80:10:10 to prepare a positive electrode and coated on the aluminum foil. The anode and electrolyte were lithium metal piece and 1 M $LiPF_6$ solution in the mixture of ethylene carbonate, ethylene methyl carbonate, and dimethyl carbonate (1/1/1 by volume ratio). The galvanostatic charge and discharge tests were implemented on LAND battery test system between 2.0 and 4.8 V (1 C = 250 mAh g^{-1}). Autolab PGSTAT 128 N electrochemical workstation was used to measure cyclic voltammetry (CV) and electrochemical impedance spectroscopy (EIS) tests.

3 Results and discussion

The XRD patterns of the samples are shown in Fig. 1. As shown in the figure, the patterns of as-synthesized LNO are consistent with standard LNO diffraction pattern (JCPDF#20-0631). Furthermore, the XRD patterns of all samples are indexed to a hexagonal α-$NaFeO_2$ structure with R-3 m group space, implying that all samples have a typical layered structure [13, 14]. The minor diffraction peaks between 20° and 25° indicate the Li_2MnO_3-like unit cell with monoclinic (C2/m) symmetry, which is a typical feature of lithium-rich materials [15]. There are obvious split peaks between (006)/(012) and (018)/(110) peaks, which indicate that all samples have good crystallinity [16,17]. The Rietveld results for lattice parameters are listed in Table 1. In addition, the c/a ratio represented the order of cations in the layered structure [18]. The ratios of all samples were greater than 4.9, indicating a good ordered, layered structure. The 3 wt% LNO-LMNCO and 5 wt% LNO-LMNCO except for 1 wt% LNO-LMNCO clearly show standard patterns of LNO, which is due to low LNO content in 1 wt% LNO-LMNCO.

Figure 2 presents SEM images of LMNCO and 5 wt% LNO-LMNCO. Obviously, two samples appear as the micrometer sphere of the secondary particles. After LNO surface coating, the grain size of LMNCO and 5 wt% LNO-LMNCO has no obvious change. The biggest distinction is that the surface of LMNCO grains appears smooth, while the surface of LNO-LMNCO is relatively rougher than LMNCO. The results show that the rough material on the surface of LMNCO may be LNO particles.

Table 1 The Rietveld results for lattice parameters

Samples	*a* (Å)	*c* (Å)	c/a
LMNCO	2.84371	14.15422	4.97738
1 wt% LNO-LMNCO	2.84376	14.15452	4.97740
3 wt% LNO-LMNCO	2.84412	14.15641	4.97743
5 wt% LNO-LMNCO	2.84427	14.15733	4.97749

The TEM images of the LMNCO and 5 wt% LNO-LMNCO are shown in Fig. 3, and the LMNCO particles have a smooth edge with clear interference fringes extending to margin. Furthermore, the measured interplanar spacing is 0.47nm, which is consistent with the (003) fringes of the layered LMNCO structure. Moreover, these stripes are uninterrupted and fairly straight, revealing a perfect layered structure. For 5 wt% LNO-LMNCO particles, the measured interplanar spacing is 0.21nm, which corresponds to the (202) fringes of the $LiNbO_3$ structure. The results show that the surface of LMNCO has been successfully coated with a layer of LNO particles.

The galvanostatic charge/discharge curves are shown in Fig. 4a. In the first charge, all the samples exhibit a long potential plateau about 4.5 V. Due to the oxidation of Ni ions (Ni^{2+} to Ni^{4+}) and Co ions (Co^{3+} to Co^{4+}), there is a voltage plateau between 3.8

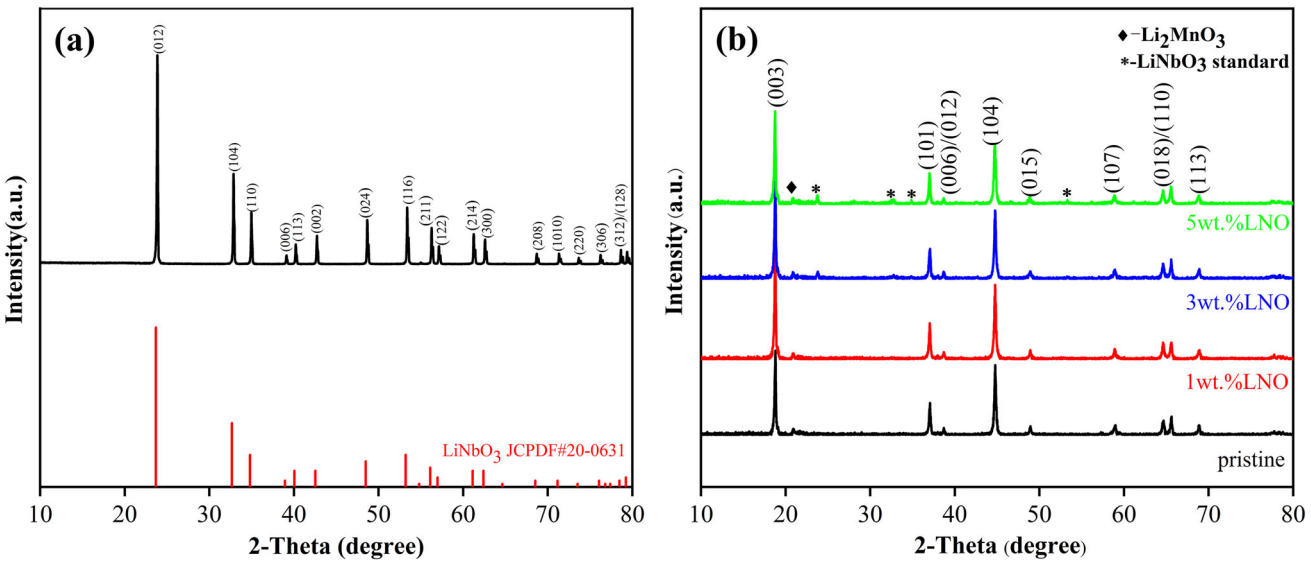

Fig. 1 The XRD pattern of the LNO (**a**). The XRD patterns of LMNCO before and after LNO surface coating (**b**)

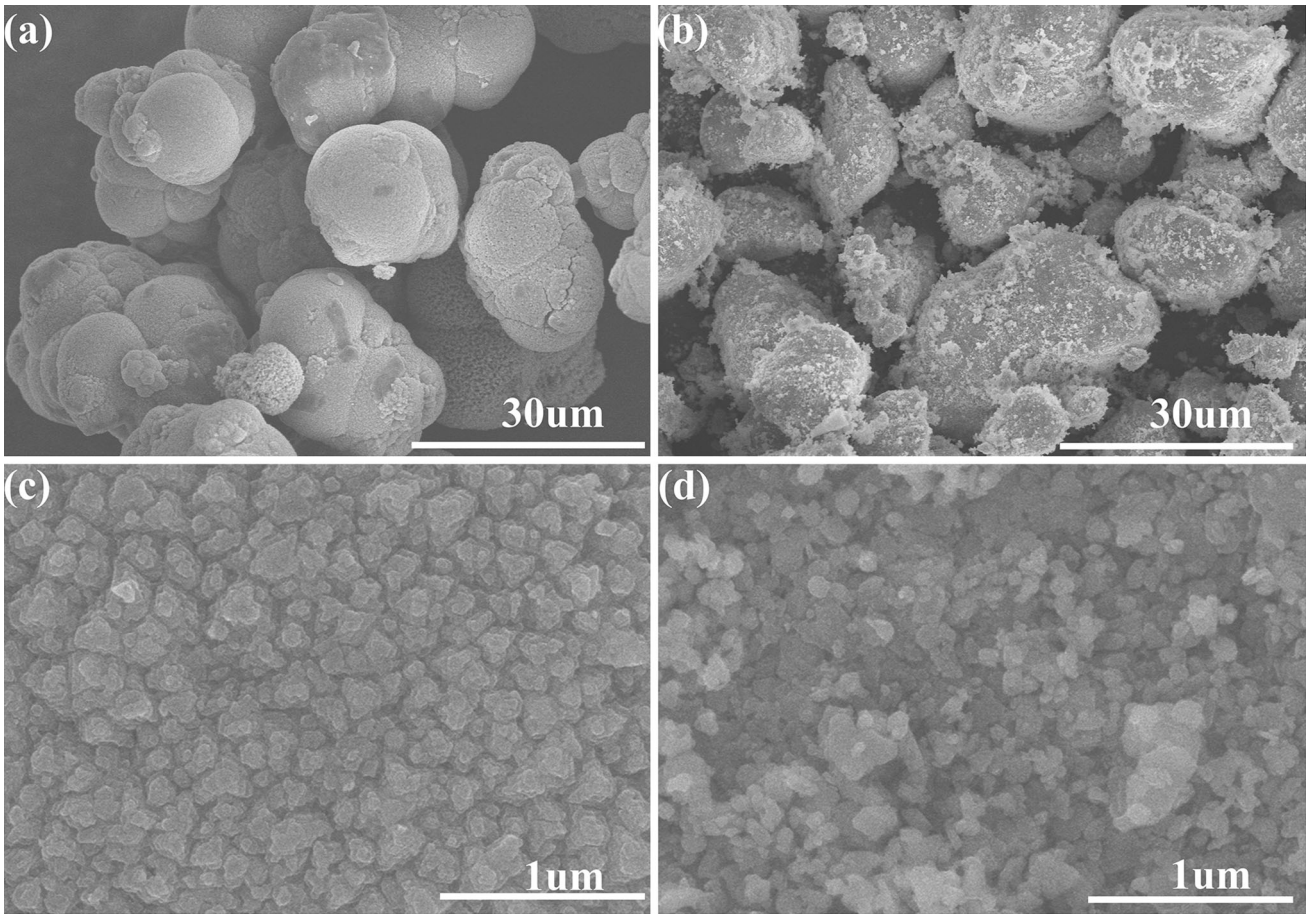

Fig. 2 SEM images of LMNCO (**a**, **c**) and 5 wt% LNO-LMNCO (**b**, **d**)

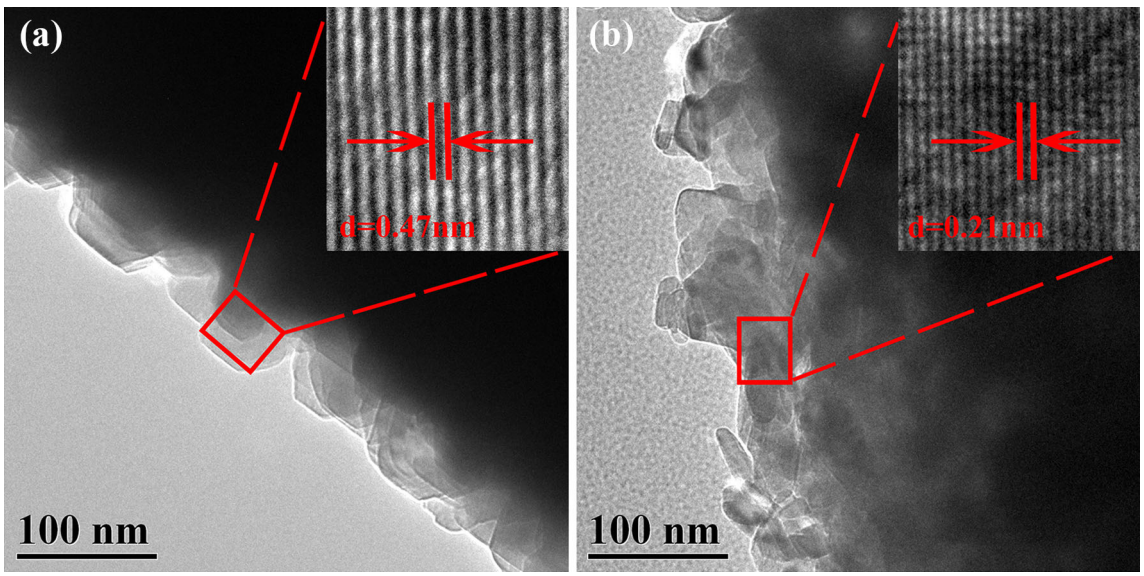

Fig. 3 TEM images of LMNCO (**a**), 5 wt% LNO-LMNCO (**b**)

and 4.2 V in the first charging curve [19], which accompanies by Li^+ deintercalation from the layered $LiMO_2$ component. Due to the irreversible extraction of lithium ions and the release of oxygen in the

Li_2MnO_3 region, and the subsequent formation of electrochemically active MnO_2, there is a long voltage plateau near 4.5 V [9, 20]. As seen in Table 2, the discharge capacity and coulombic efficiency of LMNCO, 1 wt% LNO-LMNCO, 3 wt% LNO-LMNCO, and 5 wt% LNO-LMNCO are 260.0 mAh g^{-1} and 74.2%, 264.8 mAh g^{-1} and 75.0%, 278.1 mAh g^{-1} and 77.5%, and 284.9 mAh g^{-1} and 79.1%, respectively. This implies that the LNO-coating layer with high lithium-ion diffusion rate can improve coulombic efficiency of LMNCO.

Figure 4b shows the cycle performance of all samples under 1.0 C. The initial discharge capacity of LMNCO was 212.2 mAh g^{-1}, while the capacity retention is only 70.9% after 100 cycles. While the discharge capacity and the capacity retentions of the LNO-modified samples are higher than that of LMNCO, the discharge capacity of 1wt%LNO-LMNCO, 3 wt% LNO-LMNCO, and 5 wt% LNO-LMNCO reaches 217.1, 218.3, and 218.9 mAh g^{-1}, respectively, corresponding to 82.4%, 86.9%, and 89.9% of the capacity retention rate. These results indicate that the LNO layer can prevent the direct contact of LMNCO with the electrolyte and stabilize the cathode crystal structure during cycling.

The 3rd, 10th, 25th, 50th, 75th, and 100th discharge curves of all samples are shown in Fig. 5. It can be observed that the discharge curves of all samples shift to a lower voltage platform. LMNCO exhibits severe voltage attenuation, which means greater polarization. However, LNO coating can reduce voltage attenuation of LMNCO, indicating a higher volume retention rate and a smaller polarization effect. The results show that LNO coating can effectively improve cycle stability of LMNCO.

In order to demonstrate that LNO-coating LMNCO can prevent HF corrosion, the same masses of LMNCO and 5 wt% LNO-LMNCO are added to the same volume of electrolyte. We test the content of dissolved Ni, Co, and Mn in the electrolyte by ICP-MS, and the results are shown in Table 3. Obviously, the 5 wt% LNO-LMNCO dissolves less Ni, Co, and Mn than LMNCO, which demonstrates that LNO coating can protect the cathode material from the corrosion of HF.

The rate performance of all samples at various current densities is shown in Fig. 6. It can be seen that the LNO-coated LMNCO presents better rate capacity than LMNCO during the whole testing operating. Table 4 shows the average discharge capacity of all samples at various rates. The average discharge capacity of LMNCO at 0.1, 0.2, 0.5, 1, 2, and 0.1 C is 259.8, 235.7, 220.8, 210.7, 135.1, and 239.8 mAh g^{-1}, respectively. Notably, the corresponding values of 5 wt% LNO-LMNCO increase to 285.1, 250.2, 231.5, 218.1, 156.8, and 272.4 mAh g^{-1}. The superior rate performance for the LNO layer can increase the diffusion rate of lithium ions on the surface.

The initial three cyclic voltammetry (CV) curves of LMNCO and 5 wt% LNO-LMNCO at a scan rate of 0.1 mV s^{-1} are shown in Fig. 7. In initial cycle, the oxidation peaks of LMNCO and 5 wt% LNO-

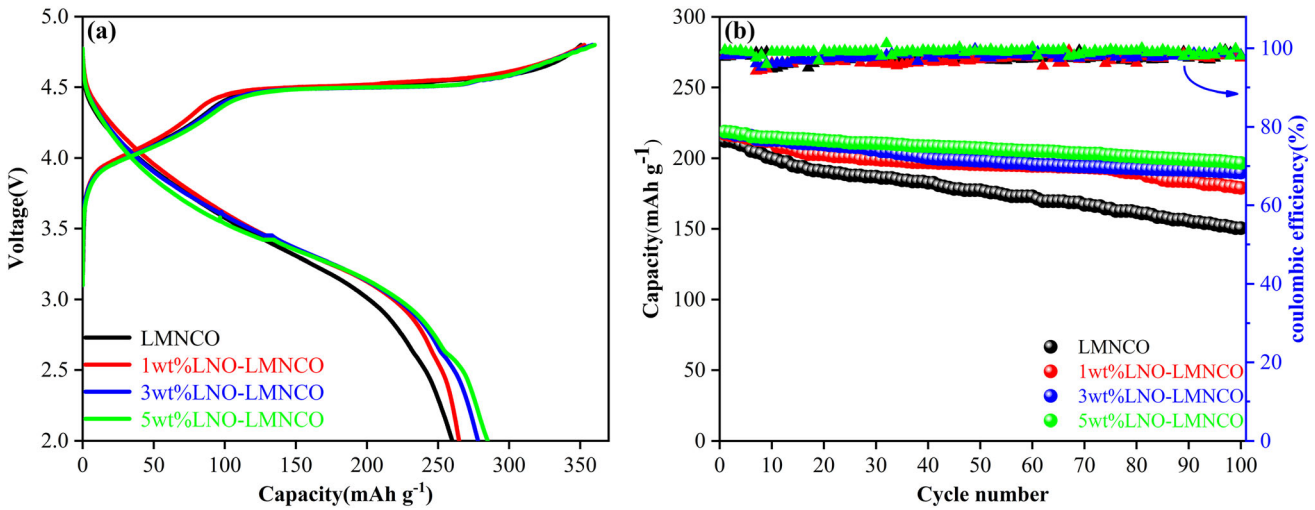

Fig. 4 Initial charge/discharge profiles of LMNCO and LNO surface coating at 0.1 C (**a**). Cycle performance of the LMNCO before and after LNO surface coating at 1.0 C (**b**)

Table 2 The initial charge/discharge capacities of LMNCO and LNO surface coating at 0.1 C

Sample	Charge capacity (mAh g^{-1})	Discharge capacity (mAh g^{-1})	Coulombic efficiency (%)
LMNCO	350.5	260.0	74.2
1 wt% LNO-LMNCO	352.9	264.8	75.0
3 wt% LNO-LMNCO	358.7	278.1	77.5
5 wt% LNO-LMNCO	360.2	284.9	79.1

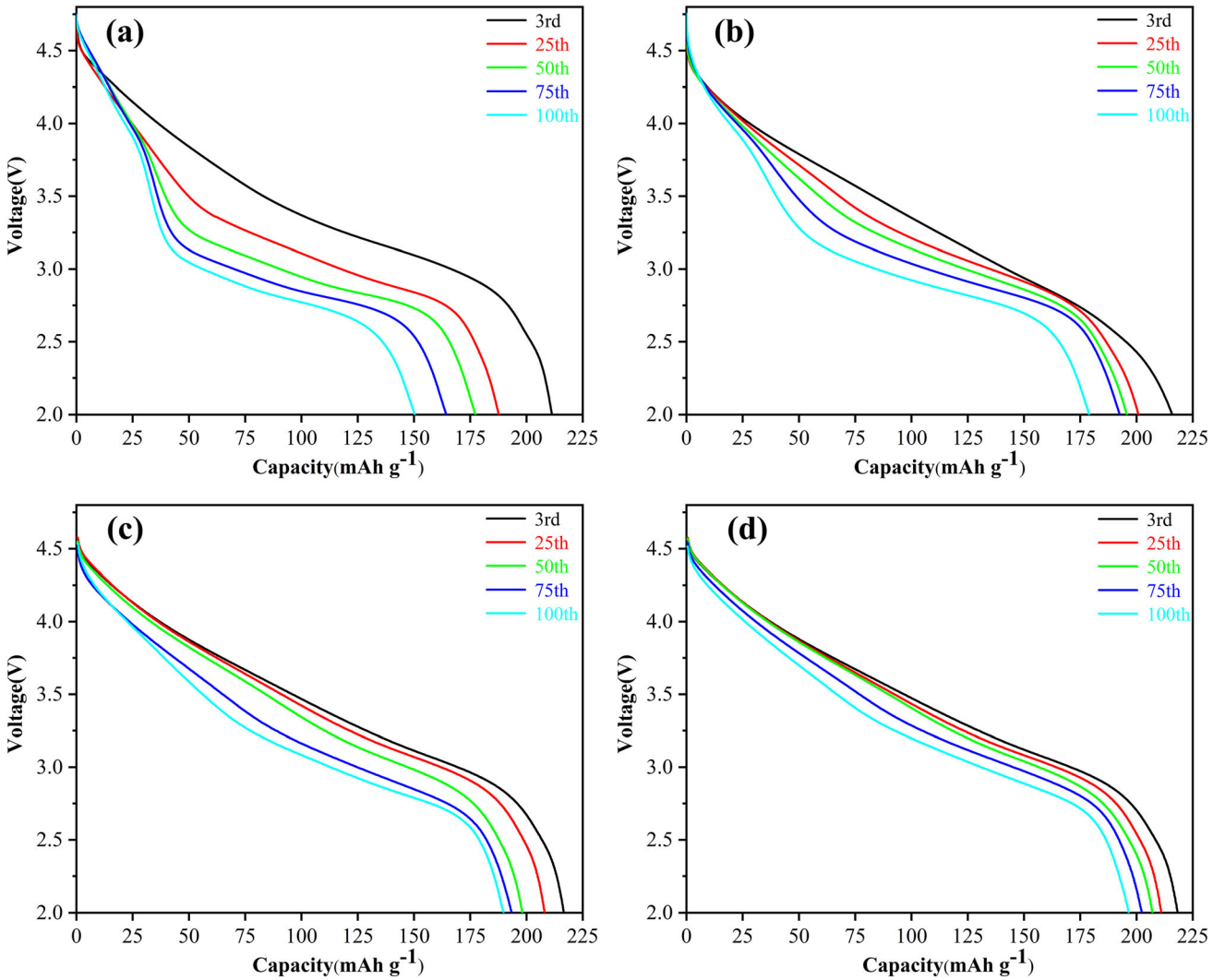

Fig. 5 Discharge curve of all samples at 1.0 C, LMNCO (**a**), 1 wt% LNO-LMNCO (**b**), 3 wt% LNO-LMNCO (**c**), and 5 wt% LNO-LMNCO (**d**)

Table 3 Concentration of Ni, Co, and Mn in electrolyte

Sample	Ni (ug mL^{-1})	Co (ug mL^{-1})	Mn (ug mL^{-1})
LMNCO	3.93	5.92	25.77
5 wt% LNO-LMNCO	1.88	2.16	10.43

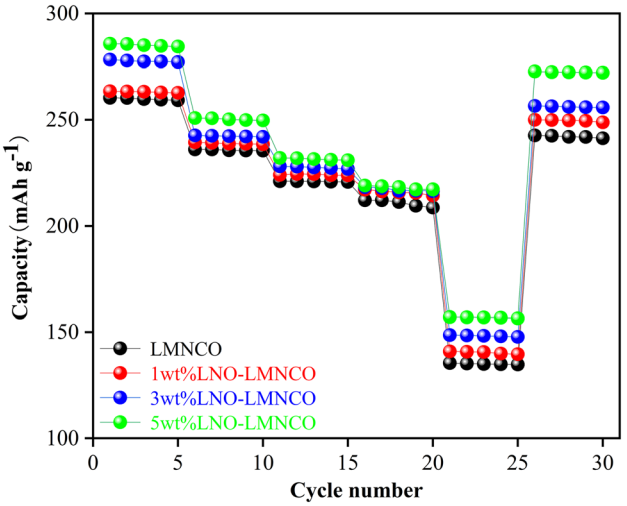

Fig. 6 Rate performance of the LMNCO before and after LNO surface coating

LMNCO are related to the oxidation of Ni (Ni^{2+} to Ni^{4+}) and Co (Co^{3+} to Co^{4+}) at ~ 4.0 V (vs. Li+/Li). The peak at ~ 4.6 V is mainly related to the irreversible reaction that strips Li_2O from the Li_2MnO_3 component to form MnO_2. Due to the reduction of Mn^{4+}, a reduction peak appears at ~ 3.2 V to balance the oxygen vacancy charge caused by the loss of oxygen in initial charge [21]. In the second scan, the other peaks near 2.88 and 2.61 V may be due to the oxidation and reduction process of Mn ions in the spinel composition between +3 and +4 states [22,23]. In subsequent scans, the reversible redox reaction of Mn component can still be observed under 3.5 V. The overlap of the curves after coating is better than that of LMNCO, which proves to have better reversibility.

The EIS test is implemented in order to deeply study the influence of lithium-ion diffusion coefficient on rate performance. The Nyquist plots of the LMNCO and 5wt%LNO-LMNCO are made up of two parts: a straight line in low-frequency region and a semicircle in high-frequency region. The high-frequency semicircle is connected with the ohmic resistance of the electrode (Rs) and the charge transfer resistance (R_{ct}) is connected with the intermediate frequency semicircle [24–26]. The illustration in Fig. 8a shows the equivalent circuit model. Table 5 shows the fitted impedance data. The linear relationship between Z′ and σ is shown in Fig. 8b. Eq. (1) is used to estimate the D_{Li+}:

$$D_{Li+} = \frac{R^2T^2}{2A^2n^4F^4C^2\sigma}, \quad (1)$$

$$Z' = R_s + R_{ct} + \sigma\omega^{-1/2}. \quad (2)$$

The ideal gas constant and Faraday constant are R (8.314J K^{-1}) and F (96485 C mol^{-1}), respectively. The surface area of the cathode and absolute temperature are defined as A (cm^2) and T (298 K). The number of transferred electrons and the concentration of lithium ions are represented by n and C. There is a linear relationship between Z′ and $\omega^{-1/2}$, and its slope is related to the Warburg factor (σ), which was related to the real impedance (Z′) in Eq. (2) [27]. The 5 wt% LNO-LMNCO has a smaller Rct value than pure LMNCO. Lithium-ion diffusion coefficients of 9.40×10^{-14} and 1.15×10^{-13} cm^2 S^{-1} were obtained for LMNCO and 5 wt% LNO-LMNCO, respectively. The results apply that the introduction of LNO into the LMNCO samples can decrease the resistance of interfaces and improve lithium ions diffusion rate, thus, achieving better rate performance.

The electrochemical performances of LMNCO are coated by various substances previously reported in the literature are shown in Table 6. Obviously, overall electrochemical performance of LNO-LMNCO is better than that of lithium-rich cathode materials coated by various materials. Especially, LNO-LMNO has higher cycle stability and capacity retention.

Table 4 Rate capacities of LMNCO before and after LNO surface coating at various rates

Sample	0.1 C (mAh g^{-1})	0.2 C (mAh g^{-1})	0.5 C (mAh g^{-1})	1 C (mAh g^{-1})	2 C (mAh g^{-1})	Back to 0.1 C (mAh g^{-1})
LMNCO	259.8	235.7	220.8	210.7	135.1	239.8
1 wt% LNO-LMNCO	263.1	238.9	224.1	215.9	140.4	248.9
3 wt% LNO-LMNCO	277.6	242.3	227.5	217.2	148.3	256.1
5 wt% LNO-LMNCO	285.1	250.2	231.5	218.1	156.8	272.4

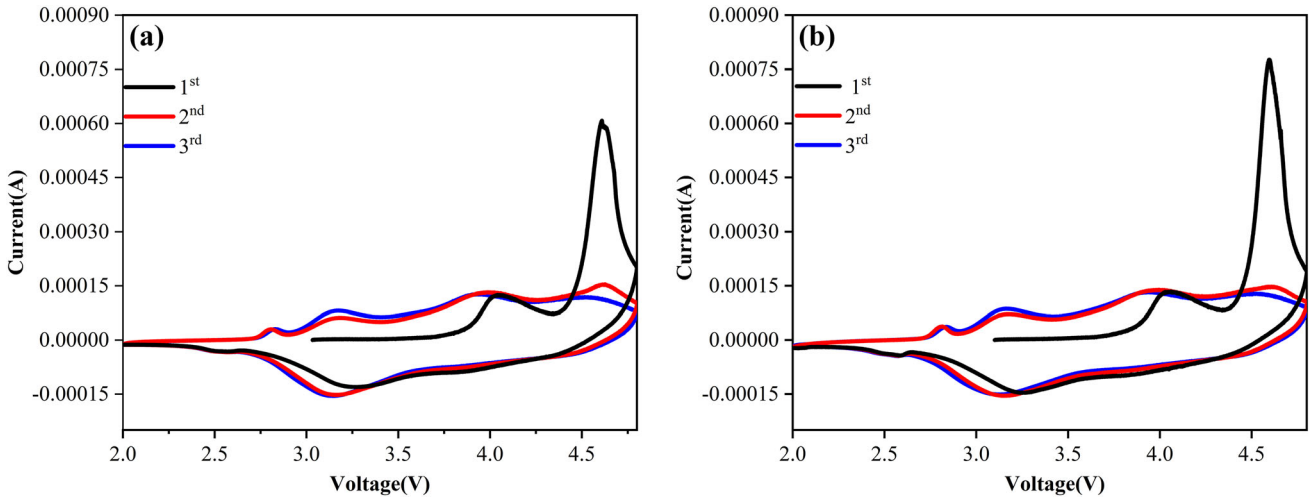

Fig. 7 CV curves of LMNCO (**a**) and 5 wt% LNO-LMNCO (**b**)

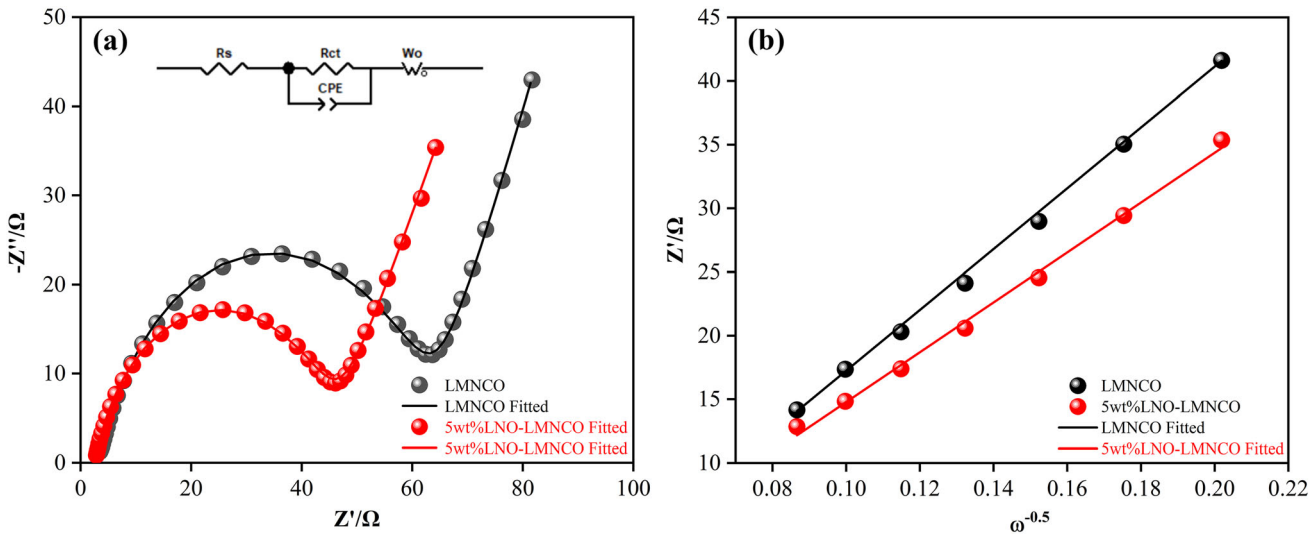

Fig. 8 Nyquist plots of LMNCO and 5 wt% LNO-LMNCO (**a**), the relationship between Z′ and $\omega^{-0.5}$ of LMNCO and 5 wt% LNO-LMNCO (**b**)

Table 5 Impedance parameters of LMNCO and 5 wt% LNO-LMNCO samples before cycling

Sample	R_s/Ω	R_{ct}/Ω	D_{Li+}/cm^2 s^{-1}
LMNCO	2.65	55.47	9.40×10^{-14}
5 wt% LNO-LMNCO	2.53	42.74	1.15×10^{-13}

4 Conclusions

In summary, the electrochemical properties of LMNCO are greatly improved by LNO-coating modification. The LNO-coating layer improves the diffusion rate of lithium ions, and availability inhibits the side reaction between electrode and electrolyte, which contributes to improving rate capacity and cycle stability of LMNCO. It is found through testing that the optimum LNO content is 5%. The 5 wt% LNO-LMNCO has a highest discharge capacity (284.9 mAh g^{-1}) and coulombic efficiency (79.09%) under 0.1 C. Besides, it reveals a higher capacity retention of 89.9% (vs. 70.9% of LMNCO) with a high discharge capacity of 180.2 mA h g^{-1} (vs. 149.3 mA h g^{-1} of LMNCO) after 100 cycles under 1.0 C. Therefore, the surface modification with LNO is an effective way to improve the electrochemical properties of LMNCO.

Table 6 Comparison of electrochemical performances of various substances-coated LMNCO reported in the literature

Coater	Discharge capacity at 0.1 C (mAh g^{-1}), initial coulombic efficiency	Rate (C), cycle numbers, discharge capacity (mAh g^{-1}), capacity retention ratio	Ref.
LiV_3O_8	–-	1.0, 50, 144.0, 87.6%	[28]
$Li_4V_2Mn\ (PO_4)_4$	–	1.0, 100, ∼ 175.0, 87.5%	[29]
$CeAlO_8$	286.7, 76.3%	1.0, 100, ∼200.0, ∼ 88.8%	[30]
$SmPO_4$	309.5, 82.5%	1.0, 100, 189.6, 88.4%	[12]
Li_2SiO_3	275.1, 81.3%	1.0, 100, 142.0, 85.1%	[11]
$Li_{1.13}Mn_{0.47}Ni_{0.2}Co_{0.2}O_2$	∼ 260.0, ∼ 78.8%	1.0, 100, 158.0, 93.0%	[31]
SnO_2	264.6, ∼ 80.1%	1.0, 100, ∼190.0, ∼92.6%	[32]
LaNiO3	285.1, 70.0%	1.0, 50, 190.3, 92.0%	[33]
$LiCeO_2$	–	1.0, 100, ∼200.0, ∼88.9%	[34]
YOF	250.4, 76.6%	1.0, 100, 157.3, 85.6%	[35]
Al_2O_3/SiO_2	281.1, 84.6%	1.0, 100, ∼185.0, 86.0%	[36]
$Li_{1.5}Na_{0.5}SiO_3$	280.9, ∼ 80.2%	0.5, 100, 190.4, 85.0%	[37]
$LiAl_5O_8$	243.5, 82.6%	0.5, 100, 200.7, 83.5%	[38]
ZrF_4	271.3, 78.8%	0.5, 100, 195.4, 91.9%	[39]
TiO_2	276.5, 80.8%	0.5, 100, ∼200.0, 88.9%	[40]
LaF_3	276.5, 80.8%	0.5, 100, ∼200.0, 88.9%	[41]
This work	284.9, 79.1%	1.0, 50, 207.1, 94.6% 1.0, 100, 196.8, 89.9%	

Funding

This work received support from the Chongqing Technology Innovation and Application Development project of Chongqing Science and Technology Commission (No.cstc2019jscx-msxmX0358), the Key Project of Science and Technology Research of Chongqing Education Commission of China (No.KJZDK201801103), the Scientific and Technological Research Foundation of Chongqing Municipal Education Commission (No.KJQN201901110), the Venture & Innovation Support Program for Chongqing Overseas Returnees (No.cx2019128), and the General program of Chongqing Natural Science Foundation (No.cstc2019jcyj-msxmX0165).

Declarations

Conflict of interest There are no conflicts to declare.

References

1. M.H. Sun, S.Z. Huang, L.H. Chen, Y. Li, X.Y. Yang, Z.Y. Yuan, B.L. Su, Applications of hierarchically structured porous materials from energy storage and conversion, catalysis, photocatalysis, adsorption, separation, and sensing to biomedicine. Chem. Soc. Rev. **45**, 3479–3563 (2016)
2. W.D. Li, B.H. Song, A. Manthiram, High-voltage positive electrode materials for lithium-ion batteries. Chem. Soc. Rev. **46**, 3006–3059 (2017)
3. L. Kang, M. Zhang, J. Zhang, S. Liu, N. Zhang, W. Yao, Y. Ye, C. Luo, Z. Gong, C. Wang, X. Zhou, X. Wu, S.C. Jun, Dual-defect surface engineering of bimetallic sulfide nanotubes towards flexible asymmetric solid-state supercapacitors. J. Mater. Chem. A **8**, 24053–24064 (2020)
4. L. Kang, C. Huang, J. Zhang, M. Zhang, N. Zhang, S. Liu, Y. Ye, C. Luo, Z. Gong, C. Wang, X. Zhou, X. Wu, S.C. Jun, Effect of fluorine doping and sulfur vacancies of $CuCo_2S_4$ on its electrochemical performance in supercapacitors. Chem. Eng. J. **390**(2020)
5. S. Liu, L. Kang, J. Hu, E. Jung, J. Zhang, S.C. Jun, Y. Yamauchi, Unlocking the potential of oxygen-deficient copper-doped Co_3O_4 nanocrystals confined in carbon as an advanced electrode for flexible solid-state supercapacitors. ACS Energy Lett. **6**, 3011–3019 (2021)
6. M.M. Thackeray, S.H. Kang, C.S. Johnson, J.T. Vaughey, R. Benedek, S.A. Hackney, Li_2MnO_3-stabilized $LiMO_2$ (M = Mn, Ni, Co) electrodes for lithium-ion batteries. J. Mater. Chem. **17**, 3112–3125 (2007)
7. H. Arai, S. Okada, Y. Sakurai, J. Yamaki, Reversibility of $LiNiO_2$ cathode. Solid State Ion. **95**, 275–282 (1997)
8. M. Gu, I. Belharouak, J.M. Zheng, H.M. Wu, J. Xiao, A. Genc, K. Amine, S. Thevuthasan, D.R. Baer, J.G. Zhang, N.D. Browning, J. Liu, C.M. Wang, Formation of the spinel

phase in the layered composite cathode used in Li-ion batteries. ACS Nano **7**, 760–767 (2013)
9. D. Mohanty, S. Kalnaus, R.A. Meisner, K.J. Rhodes, J.L. Li, E.A. Payzant, D.L. Wood, C. Daniel, Structural transformation of a lithium-rich $Li_{1.2}Co_{0.1}Mn_{0.55}Ni_{0.15}O_2$ cathode during high voltage cycling resolved by in situ X-ray diffraction. J. Power Sources **229**, 239–248 (2013)
10. M.K. Shobana, Metal oxide coated cathode materials for Li ion batteries—a review. J. Alloys Compd. **802**, 477–487 (2019)
11. L. Zhou, Y.N. Wu, J. Huang, X. Fang, T. Wang, W.M. Liu, Y. Wang, Y. Jin, X.C. Tang, Enhanced electrochemical performance of $Li_{1.2}Mn_{0.54}Ni_{0.13}Co_{0.13}O_2$ cathode material coated with Li^+-conductive Li_2SiO_3 for lithium ion batteries. J. Alloys Compd. **724**, 991–999 (2017)
12. L. He, J.M. Xu, T. Han, H. Han, Y.J. Wang, J. Yang, J.R. Wang, W.K. Zhu, C.J. Zhang, Y.H. Zhang, $SmPO_4$-coated $Li_{1.2}Mn_{0.54}Ni_{0.13}Co_{0.13}O_2$ as a cathode material with enhanced cycling stability for lithium ion batteries. Ceram. Int. **43**, 5267–5273 (2017)
13. Y. Li, C. Wu, Y. Bai, L. Liu, H. Wang, F. Wu, N. Zhang, Y.F. Zou, Hierarchical mesoporous lithium-rich $LiLi_{0.2}Ni_{0.2}Mn_{0.6}O_2$ cathode material synthesized via ice templating for lithium-ion battery. ACS Appl. Mater. Interfaces **8**, 18832–18840 (2016)
14. K. Redel, A. Kulka, A. Plewa, J. Molenda, High-performance Li-rich layered transition metal oxide cathode materials for Li-ion batteries. J. Electrochem. Soc. **166**, A5333–A5342 (2019)
15. R.Z. Yu, Z.J. Zhang, S. Jamil, J.C. Chen, X.H. Zhang, X.Y. Wang, Z.H. Yang, H.B. Shu, X.K. Yang, Effects of nanofiber architecture and antimony doping on the performance of lithium-rich layered oxides: enhancing lithium diffusivity and lattice oxygen stability. ACS Appl. Mater. Interfaces **10**, 16561–16571 (2018)
16. Y.B. Cao, X.Y. Qi, K.H. Hu, Y. Wang, Z.G. Gan, Y. Li, G.R. Hu, Z.D. Peng, K. Du, Conductive polymers encapsulation to enhance electrochemical performance of Ni-rich cathode materials for Li-ion batteries. ACS Appl. Mater. Interfaces **10**, 18270–18280 (2018)
17. G.R. Hu, X.Y. Qi, K.H. Hu, X.W. Lai, X. Zhang, K. Du, Z.D. Peng, Y.B. Cao, A facile cathode design with a $LiNi_{0.6}Co_{0.2}Mn_{0.2}O_2$ core and an AlF3-activated $Li_{1.2}Ni_{0.2}Mn_{0.6}O_2$ shell for Li-ion batteries. Electrochim. Acta **265**, 391–399 (2018)
18. S.L. Pang, M. Zhu, K.J. Xu, X.Q. Shen, H.R. Wen, Y.J. Su, G.M. Yang, X. Wu, S.W. Li, W.Z. Wang, X.M. Xi, H.B. Wang, Enhanced electrochemical performance of $Li_{1.2}Mn_{0.54}Ni_{0.13}Co_{0.13}O_2$ via L-ascorbic acid-based treatment as cathode material for Li-ion batteries. J. Electrochem. Soc. **165**, A1897–A1902 (2018)
19. L. Li, B.H. Song, Y.L. Chang, H. Xia, J.R. Yang, K.S. Lee, L. Lu, Retarded phase transition by fluorine doping in Li-rich layered $Li_{1.2}Mn_{0.54}Ni_{0.13}Co_{0.13}O_2$ cathode material. J. Power Sources **283**, 162–170 (2015)
20. X.D. Xiang, W.S. Li, Self-directed chemical synthesis of lithium-rich layered oxide Li $Li_{0.2}Ni_{0.2}Mn_{0.6}O_2$ with tightly interconnected particles as cathode of lithium ion batteries with improved rate capability. Electrochim. Acta **127**, 259–265 (2014)
21. Q.Y. Wang, J. Liu, A.V. Murugan, A. Manthiram, High capacity double-layer surface modified $LiLi_{0.2}Mn_{0.54}Ni_{0.13}Co_{0.13}O_2$ cathode with improved rate capability. J. Mater. Chem. **19**, 4965–4972 (2009)
22. F. Wu, N. Li, Y.F. Su, L.J. Zhan, L.Y. Bao, J. Wang, L. Chen, Y. Zheng, L.Q. Dai, J.Y. Peng, S. Chen, Ultrathin spinel membrane-encapsulated layered lithium-rich cathode material for advanced Li-ion batteries. Nano Lett. **14**, 3550–3555 (2014)
23. J.C. Zhang, R. Gao, L.M. Sun, Z.Y. Li, H. Zhang, Z.B. Hu, X.F. Liu, Understanding the effect of an in situ generated and integrated spinel phase on a layered Li-rich cathode material using a non-stoichiometric strategy. Phys. Chem. Chem. Phys. **18**, 25711–25720 (2016)
24. T.F. Yi, Y.M. Li, S.Y. Yang, Y.R. Zhu, Y. Xie, Improved cycling stability and fast charge-discharge performance of cobalt-free lithium-rich oxides by magnesium-doping. ACS Appl. Mater. Interfaces **8**, 32349–32359 (2016)
25. T.-F. Yi, X. Han, S.-Y. Yang, Y.-R. Zhu, Enhanced electrochemical performance of Li-rich low-Co $Li_{1.2}Mn_{0.56}Ni_{0.16}Co_{0.08-x}Al_xO_2$ ($0 \le x \le 0.08$) as cathode materials. Sci. China Mater. **59**, 618–628 (2016)
26. T.-F. Yi, B. Chen, Y.-R. Zhu, X.-Y. Li, R.-S. Zhu, Enhanced rate performance of molybdenum-doped spinel $LiNi_{0.5}Mn_{1.5}O_4$ cathode materials for lithium ion battery. J. Power Sources **247**, 778–785 (2014)
27. S.Y. Yang, X.Y. Wang, X.K. Yang, Y.S. Bai, Z.L. Liu, H.B. Shu, Q.L. Wei, Determination of the chemical diffusion coefficient of lithium ions in spherical $LiNi_{0.5}Mn_{0.3}Co_{0.2}O_2$. Electrochim. Acta **66**, 88–93 (2012)
28. C.S. Xu, H.T. Yu, C.F. Guo, Y. Xie, N. Ren, T.F. Yi, G.X. Zhang, Surface modification of $Li_{1.2}Mn_{0.54}Ni_{0.13}Co_{0.13}O_2$ via an ionic conductive LiV_3O_8 as a cathode material for Li-ion batteries. Ionics **25**, 4567–4576 (2019)
29. S.Q. Yang, P.B. Wang, H.X. Wei, L.B. Tang, X.H. Zhang, Z.J. He, Y.J. Li, H. Tong, J.C. Zheng, $Li_4V_2Mn(PO_4)_4$-stablized $LiLi_{0.2}Mn_{0.54}Ni_{0.13}Co_{0.13}O_2$ cathode materials for lithium ion batteries. Nano Energy **63**(2019)

30. J. Duan, W. Tang, R. Wang, X. Tang, J. Li, M. Tang, P. Li, Inhibited voltage decay and enhanced electrochemical performance of the Li-rich layered $Li_{1.2}Mn_{0.54}Ni_{0.13}Co_{0.13}O_2$ cathode material by CeAlOδ surface coating modification. Appl. Surf. Sci. **521**(2020)
31. L. Zhao, Y. Sun, K. Song, F. Ding, Enhanced electrochemical performance of Li-rich $Li[Li_{0.2}Mn_{0.52}Ni_{0.13}Co_{0.13}V_{0.02}]O_2$ cathode materials for lithium ion batteries by $Li_{1.13}Mn_{0.47}Ni_{0.2}Co_{0.2}O_2$ coating. Ionics **26**, 4455–4462 (2020)
32. C. Chen, T.F. Geng, C.Y. Du, P.J. Zuo, X.Q. Cheng, Y.L. Ma, G.P. Yin, Oxygen vacancies in SnO_2 surface coating to enhance the activation of layered Li-Rich $Li_{1.2}Mn_{0.54}Ni_{0.13}Co_{0.13}O_2$ cathode material for Li-ion batteries. J. Power Sources **331**, 91–99 (2016)
33. X.D. Zhang, J.J. Hao, L.C. Wu, Z.M. Guo, Z.H. Ji, J. Luo, C.G. Chen, J.F. Shu, H.M. Long, F. Yang, A.A. Volinsky, Enhanced electrochemical performance of perovskite $LaNiO_3$ coating on $Li_{1.2}Mn_{0.54}Ni_{0.13}Co_{0.13}O_2$ as cathode materials for Li-ion batteries. Electrochim. Acta **283**, 1203–1212 (2018)
34. Y. Liu, Z. Yang, J. Zhong, J. Li, R. Li, Y. Yu, F. Kang, Surface-functionalized coating for lithium-rich cathode material to achieve ultra-high rate and excellent cycle performance. ACS Nano **13**, 11891–11900 (2019)
35. Y.X. Hao, F.N. Yang, D.D. Luo, J.H. Tian, Z.Q. Shan, Improved electrochemical performances of yttrium oxyfluoride-coated $LiLi_{0.2}Mn_{0.54}Ni_{0.13}Co_{0.13}O_2$ for lithium ion batteries. J. Energy Chem. **27**, 1239–1246 (2018)
36. W.X. Zhang, Y.T. Liu, J.L. Wu, H.X. Shao, Y.F. Yang, Surface modification of $Li_{1.2}Mn_{0.54}Ni_{0.13}Co_{0.13}O_2$ cathode material with Al_2O_3/SiO_2 composite for lithium-ion batteries. J. Electrochem. Soc. **166**, A863–A872 (2019)
37. X. Nie, Z. Xu, L. Chen, J. Li, J. Cheng, Q. Sun, Y. Qiao, X. Xu, Y. Zhang, D. Li, R. Peng, L. Ci, Enhanced electrochemical performance of $Li_{1.2}[Mn_{0.54}Co_{0.13}Ni_{0.13}]O_2$ enabled by synergistic effect of $Li_{1.5}Na_{0.5}SiO_3$ modification. Adv. Mater. Interfaces **7**, 2000378 (2020)
38. F. Yang, S.Z. Lin, Z.M. Guo, Y.R. Shao, B. Zhang, X.D. Zhang, S.H. Yan, A.A. Volinsky, Suppressed voltage decay and improved electrochemical performance by coating $LiAl_5O_8$ on the surface of $Li_{1.2}Mn_{0.54}Ni_{0.13}Co_{0.13}O_2$. J. Alloys Compd. **805**, 1034–1043 (2019)
39. Y.X. Zuo, B. Huang, C.M. Jiao, R.G. Lv, G.C. Liang, Enhanced electrochemical properties of $LiLi_{0.2}Mn_{0.54}Ni_{0.13}Co_{0.13}O_2$ with ZrF_4 surface modification as cathode for Li-ion batteries. J. Mater. Sci.-Mater. Electron. **29**, 524–534 (2018)
40. C. Song, W. Feng, Z. Shi, Z. Huang, Coating TiO_2 on lithium-rich $Li_{1.2}Mn_{0.54}Ni_{0.13}Co_{0.13}O_2$ material to improve its electrochemical performance. Ionics **27**, 457–468 (2020)
41. C.D. Li, Z.L. Yao, J. Xu, P. Tang, X. Xiong, Surface-modified $LiLi_{0.2}Mn_{0.54}Ni_{0.13}Co_{0.13}O_2$ nanoparticles with LaF_3 as cathode for Li-ion battery. Ionics **23**, 549–558 (2017)